Requirement for the synaptic protein interaction site for reconstitution of synaptic transmission by P/Q-type calcium channels

Sumiko Mochida*, Ruth E. Westenbroek†, Charles T. Yokoyama†, Huijun Zhong†, Scott J. Myers†, Todd Scheuer†, Kanako Itoh*, and William A. Catterall†‡

*Department of Physiology, Tokyo Medical University, Tokyo 160-8402, Japan; and †Department of Pharmacology, University of Washington, Seattle, WA 98195-7280

Contributed by William A. Catterall, December 23, 2002

$Ca_v2.1$ channels, which conduct P/Q-type Ca^{2+} currents, were expressed in superior cervical ganglion neurons in cell culture, and neurotransmission initiated by these exogenously expressed Ca^{2+} channels was measured. Deletions in the synaptic protein interaction (synprint) site in the intracellular loop between domains II and III of $Ca_v2.1$ channels reduced their effectiveness in synaptic transmission. Surprisingly, this effect was correlated with loss of presynaptic localization of the exogenously expressed channels. $Ca_v1.2$ channels, which conduct L-type Ca^{2+} currents, are ineffective in supporting synaptic transmission, but substitution of the synprint site from $Ca_v2.1$ channels in $Ca_v1.2$ was sufficient to establish synaptic transmission initiated by L-type Ca^{2+} currents through the exogenous $Ca_v1.2$ channels. Substitution of the synprint site from $Ca_v2.2$ channels, which conduct N-type Ca^{2+} currents, was even more effective than $Ca_v2.1$. Our results show that localization and function of exogenous Ca^{2+} channels in nerve terminals of superior cervical ganglion neurons require a functional synprint site and suggest that binding of soluble NSF attachment protein receptor (SNARE) proteins to the synprint site is a necessary permissive event for nerve terminal localization of presynaptic Ca^{2+} channels.

Electrophysiological and pharmacological studies have defined a diverse array of native Ca^{2+} currents having different functions in neurons (1, 2). Voltage-gated Ca^{2+} channels are complexes of a pore-forming α_1 subunit with associated $\alpha_2\delta$, β, and γ subunits (3–5). $Ca_v2.1$ channels that conduct P/Q-type Ca^{2+} currents and $Ca_v2.2$ channels that conduct N-type Ca^{2+} currents are the primary initiators of fast synaptic transmission in vertebrate neurons (1, 6–12). These Ca^{2+} channels bind directly to soluble NSF attachment protein (SNAP) receptor (SNARE) proteins involved in neurotransmitter release through a synaptic protein interaction (synprint) site in the large intracellular loop connecting domains II and III ($L_{II\text{-}III}$) of their α_1 subunits (13–15). Disruption of this interaction by peptide inhibitors injected into presynaptic neurons reduces the efficiency of Ca^{2+} entry in stimulating exocytosis (16, 17). These results implicate the interaction of SNARE proteins with the synprint site in determining the efficiency of fast synaptic transmission, possibly by organizing docked synaptic vesicles close to the site of Ca^{2+} entry.

The molecular basis for the specific role of Ca_v2 channels in initiation of fast neurotransmission is not well understood. It may involve specific localization of Ca_v2 channels in nerve terminals, specific interactions with SNARE proteins or other proteins in the nerve terminal, or both. Results presented in the accompanying paper (18) show that exogenous $Ca_v2.1$ channels can be functionally expressed in superior cervical ganglion neurons (SCGNs) and can reconstitute synaptic transmission in neurons whose endogenous $Ca_v2.2$ channels have been blocked by ω-conotoxin GVIA. Here we use this method to analyze the role of the synprint site of Ca_v2 channels in reconstitution of synaptic transmission in SCGNs. Our results reveal an unexpected requirement for the synprint site for localization and function of calcium channels in nerve terminals.

Experimental Procedures

Construction of Mutant $Ca_v2.1$ Channels. Mutations in the synprint domain of $Ca_v2.1$ were constructed from the rbA-I cDNA clone in the vertebrate expression vector pMT2 (kindly provided by T. P. Snutch, University of British Columbia, Vancouver), by using a 2,966-bp *Xho*I–*Sgr*AI fragment that encodes the N-terminal half (NT) of $Ca_v2.1$ in pUC19 (New England Biolabs) having a modified polylinker with *Xho*I and *Sgr*AI sites replacing the *Eco*RI/*Hind*III linker. After mutagenesis by loop-out deletion and confirmation of cDNA sequence, the isolated clones were digested with *Xho*I/*Sgr*AI and inserted into *Xho*I/*Sgr*AI-digested rbA-I/pMT2.

$Ca_v2.1$ containing the synprint site from $Ca_v2.2$ was constructed by replacement of amino acid residues 747–981 of $Ca_v2.1$ with amino acid residues 741–951 of $Ca_v2.2$ in PUC19/rbA-NT (see above) that was modified at the 3 *Sgr*AI insert boundary to create a dual-specific Pin AI/*Sgr*AI-compatible site, to circumvent an internal *Sgr*AI site in the $Ca_v2.2$ synprint region.

$Ca_v1.2$ containing the synprint site from $Ca_v2.1$ was constructed by PCR amplification and insertion of cDNA encoding amino acid residues 771–971 from $L_{II\text{-}III}$ of the rbA isoform of $\alpha_1 2.1$ into $\alpha_1 1.2$ at a natural PshA I restriction site (amino acid residue 837, nucleotide 2986 from the initiating ATG codon of rbC-II; ref. 19).

Cell Transfection, Membrane Extraction, and Immunoblotting. Plasmid cDNA for Ca^{2+} channel α_1, $\alpha_2\delta$, and $\beta 1b$ subunits, and enhanced GFP reporter (EGFP-N1, CLONTECH) were combined in a 1:1:1:0.1 molar ratio (60 μg total DNA for each 150-mm culture plate) and incubated with the cells for 16 h at 37°C and 3% CO_2, followed by one wash in PBS and further incubation at 5% CO_2 for 2 days. For membrane isolation, all work was carried out as rapidly as possible at 4°C with samples on ice and containing the protease inhibitors PMSF (0.2 mM), 4-(2-aminoethyl)benzenesulfonyl fluoride (AEBSF, 0.1 μg/ml), pepstatin A (1 μM), leupeptin (1 μg/ml), aprotinin (2 μg/ml), benzamidine (0.1 mM), and calpain inhibitors I and II (8 μg/ml). Plates were washed two times with 10 ml of ice-cold PBS, and cells from each plate were scraped into 2 ml of 50 mM Tris·HCl, pH 8.0, and lysed with 10 strokes at ≈1,000 rpm in a glass-teflon homogenizer. The lysate was separated by centrifugation for 5 min at 1,600 rpm in a JA-20 rotor/Beckman J2-21 centrifuge. The supernatant (S1) was trans-

Abbreviations: SNAP, soluble NSF attachment protein; SNARE, SNAP receptor; synprint; synaptic protein interaction; EPSP, excitatory postsynaptic potential; SCGN, superior cervical ganglion neuron.

‡To whom correspondence should be addressed. E-mail: wcatt@u.washington.edu.

NEUROSCIENCE

ferred to ultracentrifuge tubes and membranes sedimented for 45 min at 100,000 × *g* in a 70Ti rotor/Beckman L8-M centrifuge. The cytoplasmic fraction (S2) was stored at −80°C, whereas the membrane pellet (P2) was resuspended in 1 ml of 20 mM Tris-HCl, pH 7.4/150 mM NaCl/1% Triton X-100 (TBS/1% Triton X-100), homogenized as described above, and unsolubilized material was sedimented for an additional 30 min at 100,000 × *g*. Solubilized membranes (S3) were aliquoted and stored at −80°C for use within 1 week.

Transfection efficiency was evaluated in control studies via relative EGFP fluorescence (488 nm excitation; 509 nm emission) in the cytoplasmic fraction (S2), and confirmed equivalent efficiency of transfection among samples within the same experiment. Samples (90 μg protein) for SDS/PAGE were solubilized in SDS sample buffer, separated on a 3% stacking gel and 6% resolving gel in a Laemmli Tris-glycine buffer system (20) with MultiMark prestained molecular mass standards (NOVEX, San Diego), and electrotransferred to 0.2 μM pore nitrocellulose (Schleicher and Schuell, Keene, NH). For immunoblotting, all incubations were carried out for 1 h at room temperature with gentle rotation in a buffer of 10 mM Tris·HCl, pH 8.0/150 mM NaCl/10% nonfat milk, except where noted. Nitrocellulose filters were first blocked, then incubated with affinity-purified anti-CNA4 at 200 ng/μl. Blots were then washed three times for 5 min each, incubated with protein A-HRP (Amersham Pharmacia) at a 1:1,000 dilution, washed in the same buffer without milk three times for 5 min, three times for 15 min, and twice for 30 min, followed by enhanced chemiluminescence detection and film exposure (Amersham Pharmacia).

Expression and Electrophysiological Analysis of Ca^{2+} Channels in tsA-201 Cells. TsA-201 cells were maintained in DMEM/Ham's F12 (1:1) supplemented with 10% FBS (Life Technologies, Rockville, MD) at 37°C under 10% CO_2. Cells plated in 35-mm tissue culture dishes were grown to ≈60–80% confluence and transfected by the calcium phosphate method with a total of 4 μg DNA including a 1:1 molar ratio of cDNAs encoding Ca^{2+} channel $\alpha 1$, $\alpha_2\delta$, and β1b subunits and 0.3 μg of a CD8 expression plasmid for identification of transfected cells (21). The cells were subcultured at 24 h after the transfection. At least 48 h after transfection, positive transfected cells were visually identified by labeling with CD8-antibody-coated fluorophore. Barium currents were recorded by the whole-cell patch clamp technique using a List EPC-7 amplifier and filtered at 5 kHz with an eight-pole Bessel filter. Leak and capacitance currents were measured by using hyperpolarizing pulses and subtracted by using the p/−4 method. The extracellular recording solution contained 120 mM Tris, 4 mM $MgCl_2$, and 10 mM $BaCl_2$ with the pH adjusted to 7.3 by methanesulfonic acid. The internal pipette solution consisted of 120 mM aspartic acid, 5 mM $CaCl_2$, 2 mM $MgCl_2$, 10 mM Hepes, 10 mM EGTA, and 2 mM Mg-ATP with the pH adjusted to 7.3 by CsOH.

Expression and Electrophysiological Analysis of $Ca_v2.1$ Channels in Cultured SCGNs. These methods are described in the accompanying paper (18).

Results

Functional Expression of $Ca_v2.1$ Channels with Deletions in the Synprint Site. In the preceding paper, we show that Ca_v2 family Ca^{2+} channels can effectively initiate neurotransmission, whereas Ca_v1 family channels cannot. What molecular characteristics of these Ca^{2+} channels are responsible for this difference? Comparison of the amino acid sequences and intron/exon structures of the Ca_v1 and Ca_v2 families of Ca^{2+} channels reveals that the exons encoding the synprint site in the Ca_v2 channels are missing in Ca_v1 channels (Fig. 1). Ca_v3 channels have unrelated amino acid sequences in the corresponding position (data not shown).

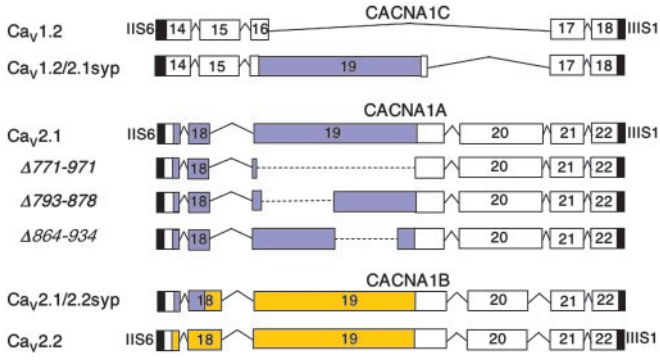

Fig. 1. Intron/exon structure, deletion mutants, and chimeras in the intracellular loop connecting domains II and III. Exons extending from transmembrane segment IIS6 to segment IIIS1 of Ca_v1 and Ca_v2 channels are aligned for comparison. Exons encoding related amino acid sequences are placed in vertical register. Amino acid sequences related to exons 19 and 20 of the Ca_v2 channels are not present in Ca_v1 channels. The synprint site of $Ca_v2.1$ is highlighted in blue and the synprint site of $Ca_v2.2$ is highlighted in yellow. The amino acid designations for the $Ca_v1.2$, $Ca_v2.1$ and $Ca_v2.2$ channels were determined from GenBank accession nos. M67515, NP_03705, and Q02294.

In view of this molecular specialization of Ca_v2 channels, we investigated the role of the synprint site in the unique ability of Ca_v2 channels to initiate synaptic transmission. The synprint site of $Ca_v2.1$ channels contains two subsites, which each can bind SNARE proteins (15). To examine the requirement for the synprint site of $Ca_v2.1$ channels for synaptic transmission, we constructed three mutant α_1 subunits with complete [$\alpha_1$2.1Δ(771–971)] or partial deletions [$\alpha_1$2.1Δ(793–878) and $\alpha_1$2.1Δ(864–934)] of the synprint site (Fig. 1, blue). These cDNAs were then expressed along with $\alpha_2\delta$ and β1b subunits in the tsA-201 subclone of human embryonic kidney HEK293 cells as described in *Experimental Procedures*. Immunoblots of extracts of these cells showed comparable expression of the wild-type and mutant channels, and immunocytochemical analysis with antibodies specific for the $Ca_v2.1$ showed comparable cellular expression and distribution of wild-type, $\alpha_1$2.1Δ(793–878), $\alpha_1$2.1Δ(864–934), and $\alpha_1$2.1Δ(771–971) (Fig. 2 *A* and *C–F*). These results show that the synprint site is not required for expression of $Ca_v2.1$ channels in mammalian cells.

The functional properties of the deletion mutants were analyzed by whole-cell voltage clamp with barium as the permeant ion (Fig. 3). The barium currents conducted by wild-type $Ca_v2.1$ channels activated rapidly and inactivated slowly as previously reported (Fig. 3*A Inset*; ref. 22). Similar barium currents were recorded for the partial deletion mutants $\alpha_1$2.1Δ(793–878) and $\alpha_1$2.1Δ(864–934). In contrast, the complete deletion of the synprint site in mutant $\alpha_1$2.1Δ(771–971) prevented functional expression of $Ca_v2.1$ in tsA-201 cells (data not shown). Thus, partial deletions that reduce but do not abolish SNARE protein binding are functionally expressed, whereas complete deletions are not. The voltage dependence of activation and inactivation of the barium currents conducted by wild-type and mutant $Ca_v2.1$ channels was similar (Fig. 3*A*).

To determine whether functional interactions with SNARE proteins were impaired by these deletion mutations, we examined the regulation of wild-type and mutant $Ca_v2.1$ channels by SNAP-25, which binds specifically to the synprint site of the rbA isoform of $Ca_v2.1$ (15) and shifts the voltage dependence of inactivation (22). Coexpression of SNAP-25 has little effect on activation but causes a significant negative shift in the voltage dependence of steady-state inactivation for wild-type $Ca_v2.1$, as reported previously (Fig. 3*B*). This functional interaction is nearly completely lost in $\alpha_1$2.1Δ(793–878) and $\alpha_1$2.1Δ(864–934)

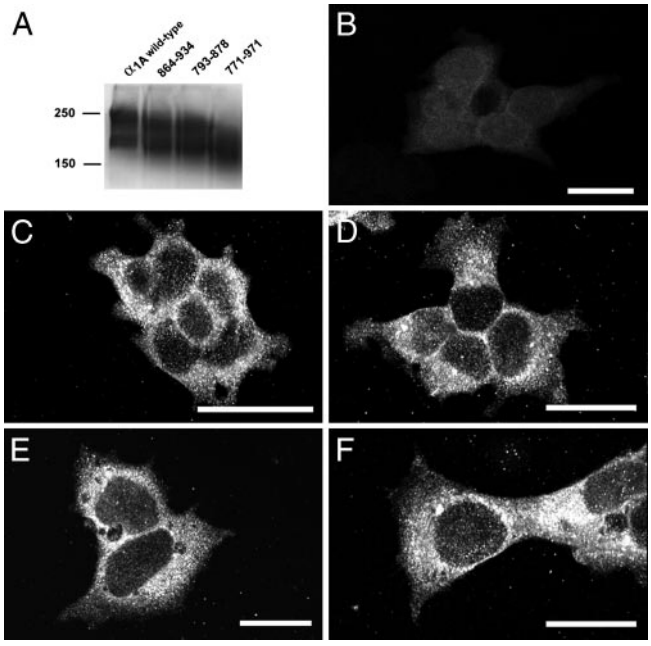

Fig. 2. Expression of $Ca_v2.1$ channels with deletions in the synprint site. (*A*) Immunoblots of expressed wild-type and mutant $Ca_v2.1$. cDNAs encoding $Ca_v2.1$ were expressed in tsA-201 cells, and immunoblotting was carried out with anti-CNA4 as described in *Experimental Procedures*. Gel lanes, from left to right, indicate transfected $Ca_v2.1$ and synprint mutants Δ(864–934), Δ(793–878), and Δ(771–971). Predicted molecular masses of $Ca_v2.1$ and mutants, from left to right, are 252, 244, 242, and 229 kDa, respectively. Dye-coupled molecular mass standards for 250-kDa myosin and 150-kDa phosphorylase B are indicated on the left. (*B–F*) Immunocytochemical analysis of expression of wild-type and mutant $Ca_v2.1$. tsA-201 cells tested under control conditions (*B*) or transfected with cDNA encoding $Ca_v2.1$ (*C*), $\alpha_1$2.1Δ(793–878) (*D*), $\alpha_1$2.1Δ(864–934) (*E*), or $\alpha_1$2.1Δ(771–971) (*F*) were stained with anti-CNA4 antibodies as described in *Experimental Procedures*.

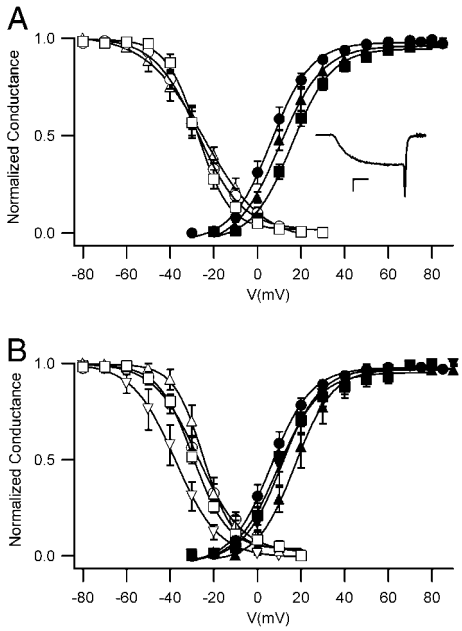

Fig. 3. Function of $Ca_v2.1$ channels with deletions in the synprint site. (*A*) Voltage dependence of gating. Activation: Ba^{2+} currents were recorded during 10-ms test pulses to the indicated potentials from holding potential of −80 mV. The cell was repolarized to −40 mV for 3 ms. Tail currents were normalized to the largest tail current in each series of test pulses, and means ± SEM were plotted as a function of test voltage. $Ca_v2.1$, filled circles (n = 12); $\alpha_1$2.1Δ(864–934), filled triangles (n = 7); $\alpha_1$2.1Δ(793–878), filled squares (n = 8). (*Inset*) A representative Ba^{2+} current recorded at +20 mV. (Calibration bars: 200 pA, 2 ms.) Inactivation. Ba^{2+} currents were recorded during a 10-ms test pulse to +30 mV from the holding potential of −80 mV. After repolarizing the cell to −80 mV for 20 ms, a 4-s conditioning prepulse to the indicated potentials was applied followed by the second test pulse of 10 ms to +30 mV. Tail currents from the second test pulse were normalized to the largest tail current in each series and plotted as mean ± SEM versus conditioning prepulse voltage. $Ca_v2.1$, open circles (n = 10); $\alpha_1$2.1Δ(793–878), open triangles (n = 3); $\alpha_1$2.1Δ(864–934), open squares (n = 7). (*B*) Effects of SNAP-25. The voltage dependence of activation and inactivation was measured as in *A* for $Ca_v2.1$, open and filled circles (n = 15); $Ca_v2.1$ with SNAP-25, open and filled inverted triangles (n = 5); $\alpha_1$2.1Δ(793–878) with SNAP-25, open and filled squares (n = 4); and $\alpha_1$2.1Δ(864–934) with SNAP-25, open and filled triangles (n = 3).

(Fig. 3*B*). Evidently deletion of either half of the synprint site is sufficient to impair functional interactions with SNAP-25.

Requirement for the Synprint Site of $Ca_v2.1$ Channels for Synaptic Transmission. Previous results show that peptides containing the synprint site of N-type Ca^{2+} channels inhibit synaptic transmission when injected into presynaptic SCGNs or motor neurons, consistent with the conclusion that interactions of the synprint site with SNARE proteins are necessary for efficient synaptic transmission (16, 17). To test the role of interactions with the synprint site of P/Q-type Ca^{2+} channels in synaptic transmission more directly, we expressed the mutant $\alpha_1$2.1 subunits in which portions of the synprint site were deleted by injection together with dextran-fluorescein beads in SCGNs. Successfully injected neurons were identified by fluorescence, and synaptic transmission to neighboring cells was measured by microelectrode impalements of pairs of neurons. The effectiveness of the different $Ca_v2.1$ channels in initiating synaptic transmission was assessed from block of synaptic transmission by agatoxin IVA. In neurons expressing $Ca_v2.1$ channels with these deletions, synaptic transmission was less sensitive to inhibition by 250 μM ω-agatoxin IVA compared with wild-type P/Q-type Ca^{2+} channels (Fig. 4). At 20 min after bath application of 250 nM ω-agatoxin IVA, only 9 ± 6% (n = 6) inhibition of excitatory postsynaptic potential (EPSP) amplitude was observed in neurons injected with $\alpha_1$2.1Δ(864–934) (Fig. 4 *A*, *E*, and *F*) or 19 ± 6% (n = 7) in neurons injected with $\alpha_1$2.1Δ(793–878) (Fig. 4 *B*, *E*, and *F*). This compares to 28 ± 8% (n = 5) inhibition of EPSPs by ω-agatoxin IVA at synapses expressing wild-type $\alpha_1$2.1 (Fig. 4 *D–F*). As a negative control we also analyzed synapses expressing $\alpha_1$2.1Δ(771–971), which lacks the entire synprint site and is functionally inactive. As expected, EPSP amplitude was not significantly reduced (6 ± 6%; n = 5) at 20 min after bath application of 250 nM ω-agatoxin IVA, consistent with the failure of this mutant to yield functional Ca^{2+} channels in tsA-201 cells (Fig. 4 *C*, *E*, and *F*). Together, these results indicate that an intact synprint site is required for evoked synchronous transmitter release initiated by opening of exogenously expressed P/Q-type Ca^{2+} channels.

Effect of Deletion of the Synprint Site on Presynaptic Localization of $Ca_v2.1$ Channels. The requirement for the synprint site of $Ca_v2.1$ channels for effective initiation of synaptic transmission could indicate an important role for this segment of the Ca^{2+} channel in presynaptic localization of these channels, an important role for the synprint site in Ca^{2+}-dependent exocytosis itself, or both. To distinguish these possibilities, we analyzed the nerve terminals of injected neurons for $Ca_v2.1$ localization in presynaptic terminals by immunocytochemistry. Surprisingly, the results reveal a requirement for the synprint site in presynaptic localization of P/Q-type Ca^{2+} channels. We used polyclonal antibodies directed against the $L_{I\text{-}II}$ (Fig. 5 *A–C*) and $L_{II\text{-}III}$

NEUROSCIENCE

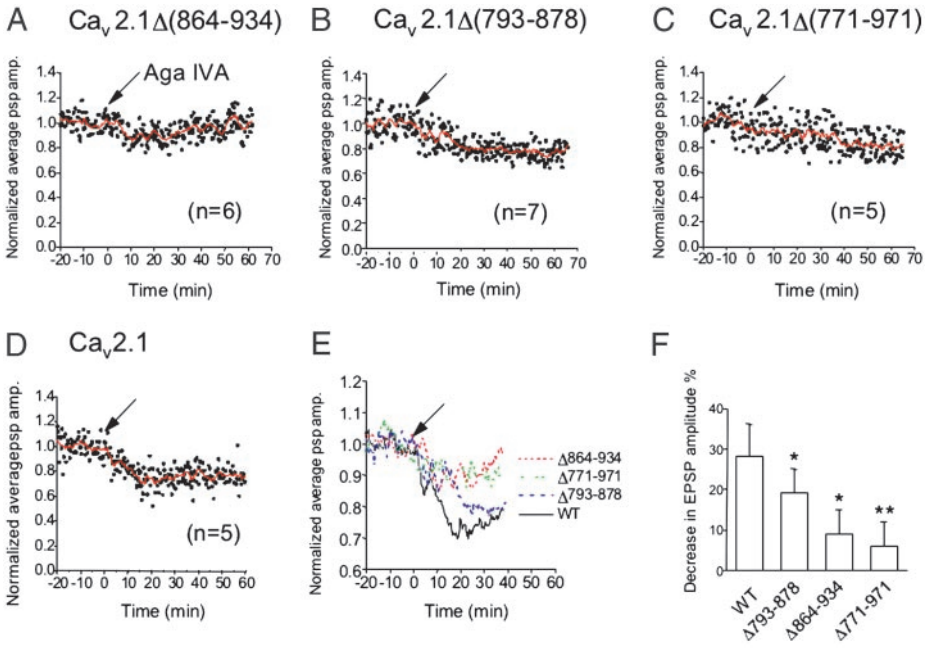

Fig. 4. Effect of ω-agatoxin IVA on synaptic transmission at synapses expressing mutant $Ca_v2.1$ channels. Synaptic transmission was recorded from pairs of SCGNs as described in *Experimental Procedures*, and ω-agatoxin IVA (250 nM) was applied at $t = 0$ (arrows). (*A*) EPSPs were recorded from synapses expressing $Ca_v2.1\Delta(864–934)$ ($n = 7$). (*B*) EPSPs were recorded from synapses expressing $Ca_v2.1\Delta(793–878)$ ($n = 6$). (*C*) EPSPs were recorded from synapses expressing $Ca_v2.1\Delta(771–971)$ ($n = 5$). (*D*) EPSPs were recorded at the synapses expressing wild-type $Ca_v2.1$ ($n = 5$). (*E*) Smoothed values of the normalized average EPSP amplitude with moving average algorithm in *A–D* were plotted against recording time. (*F*) Bar graph illustrating the mean EPSP values ± SEM at 20 min after the toxin application. *, A statistically significant difference from control at $P < 0.05$; **, $P < 0.02$.

(Fig. 5 *D–F*) intracellular loops to label cultures of SCGNs containing injected neurons. The synaptic terminals on neurons receiving innervation from adjacent injected neurons were examined for labeled puncta representing nerve terminals containing $Ca_v2.1$ (Fig. 5 *A–F*), and the numbers of puncta were counted and compared for wild-type and mutant $Ca_v2.1$ channels (Fig. 5*G*). Because only presynaptic neurons are injected, labeled puncta on adjacent neurons must represent $Ca_v2.1$ channels in presynaptic terminals and not postsynaptic clusters of $Ca_v2.1$ channels. We found that wild-type $Ca_v2.1$ channels were efficiently localized in nerve terminals (Fig. 5 *A*, *D*, and *G*). In contrast, $\alpha_1 2.1\Delta(793–878)$ was less efficiently localized in nerve terminals (Fig. 5 *B*, *E*, and *G*), and $\alpha_1 2.1\Delta(864–934)$ was not detected at all in highly labeled puncta in nerve terminals (Fig. 5 *C*, *F*, and *G*). Thus, deletion of the synprint site impairs synaptic transmission by these exogenously expressed $Ca_v2.1$ channels because they are not efficiently transported to or retained in nerve terminals. Although the deletion of the synprint site may also cause an impairment of the function of these channels in nerve terminals, the large reduction in Ca^{2+} channel density in nerve terminals effectively masks any additional effect on the efficiency of synaptic transmission by the few channels that are effectively localized.

Effect of Substitutions of the Synprint Site on Synaptic Transmission Initiated by $Ca_v1.2$ and $Ca_v2.1$. As shown in the preceding paper (18), $Ca_v1.2$ channels are not able to reconstitute synaptic transmission in SCGNs. To further define the role of the synprint site in synaptic localization and synaptic transmission, we constructed a chimeric Ca^{2+} channel in which the synprint site of $Ca_v2.1$ was inserted into $L_{II\text{-}III}$ of $Ca_v1.2$ (see *Experimental Procedures*). Because Ca_v1 family channels lack the exons encoding the synprint site and have a short $L_{II\text{-}III}$ (Fig. 1), the synprint site was added to $L_{II\text{-}III}$ of $Ca_v1.2$ rather than substituted for a corresponding segment of $Ca_v1.2$. cDNA encoding this chimera was injected into SCGNs, and synaptic transmission was measured. Remarkably, insertion of the synprint site of $Ca_v2.1$ into $Ca_v1.2$ yielded a chimeric channel that was able to support robust synaptic transmission, as indicated by a reduction of the EPSP amplitude of 28 ± 8% ($n = 5$) by bath application of 2.5 μM nifedipine, a specific blocker of L-type Ca^{2+} currents that normally has no effect on synaptic transmission (Fig. 6 *A* and *C*). In addition, the decay time constant of the EPSP was significantly shortened from 34 ± 2.5 ms to 27 ± 3.2 ms ($n = 5$). Evidently, insertion of the synprint site is sufficient to allow nerve terminal localization and function of $Ca_v1.2$, which conducts L-type Ca^{2+} currents that initiate transmitter release.

Normal synaptic transmission in SCGNs is mediated by N-type Ca^{2+} currents. Therefore, it is possible that the synprint site of $Ca_v2.2$ might be more effective than the synprint site of $Ca_v2.1$ in allowing nerve terminal localization and function. To test this idea, we constructed a chimeric Ca^{2+} channel in which the synprint site of $Ca_v2.2$ was substituted in $Ca_v2.1$ (Fig. 1). This chimeric Ca^{2+} channel was more effective in initiation of synaptic transmission than wild-type $Ca_v2.1$, as indicated by a reduction in EPSP amplitude of 37 ± 5% by agatoxin IVA compared with 28 ± 8% (Fig. 6*C*). These results suggest that the synprint site from $Ca_v2.2$ is indeed significantly more effective in establishing synaptic transmission in SCGNs. Unfortunately, although this difference in synaptic transmission is significant, it is not large enough to allow us to determine whether it is correlated with increased presynaptic localization of $Ca_v2.1$ channels by using our immunocytochemical methods, which are less precise than electrophysiological recording. Therefore, increased localization and increased functional efficacy may both contribute to the increase in synaptic transmission initiated by this chimeric channel.

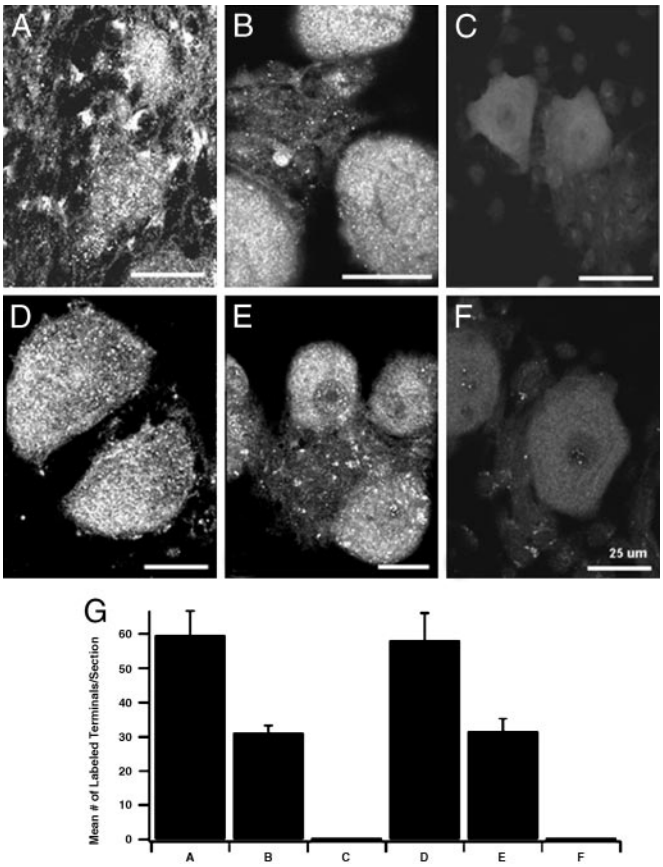

Fig. 5. Nerve terminal expression of $Ca_v2.1$ channels with deletions in their synprint sites. Injected cells labeled with fluorescein-labeled dextran sulfate were identified by confocal microscopy. The filter was then changed to view Texas red-labeled antibodies, and images of cells labeled with anti-CNA4 or anti-CNA5 that were near a cell that had been injected with wild-type or mutant $Ca_v2.1$ cDNA were collected. (*A*) $\alpha_1$2.1 labeled with anti-CNA4. (*B*) $\alpha_1$2.1Δ(793–878) labeled with anti-CNA4. (C) $\alpha_1$2.1Δ(864–934) labeled with anti-CNA4. (*D*) $\alpha_1$2.1 labeled with anti-CNA5. (*E*) $\alpha_1$2.1Δ(793–878) labeled with anti-CNA5. (*F*) $\alpha_1$2.1Δ(864–934) labeled with anti-CNA5. (*G*) Mean number of labeled puncta per section labeled with anti-CNA4 or anti-CNA5 antibodies. The numbers of puncta were counted by using the METAMORPH (Universal Imaging, Downingtown, PA) image analysis program. Error bars represent the standard error of the mean.

Discussion

The Synprint Site Is a Functional Specialization of Ca_v2 Channels. As illustrated in Fig. 1 for $Ca_v1.2$, the $L_{II\text{-}III}$ segments of Ca_v1 family of channels are much shorter than those of Ca_v2 channels, and they do not contain amino acid sequences that correspond to the synprint site. In fact, exon 19, which encodes most of the synprint site in Ca_v2 channels, is missing in the genes encoding Ca_v1 channels (Fig. 1). Similarly, the Ca_v3 channels that conduct T-type Ca^{2+} currents also have short $L_{II\text{-}III}$ segments and do not have amino acid sequences corresponding to the synprint site (data not shown). These comparisons suggest that the synprint site is a specialization of Ca_v2 channels that has developed from insertion of new exons in the evolution of the three Ca^{2+} channel families and has a specific function in synaptic transmission.

Requirement of the Synprint Site of P/Q-Type Ca^{2+} Channels for Nerve Terminal Localization and Function. Our previous results with dominant negative peptides show that interaction of the synprint site in the cytoplasmic loop connecting domains II and III of N-type Ca^{2+} channels with SNARE proteins is required for fast and synchronous neurotransmitter release from SCGNs in culture (16). This interaction also transmits a voltage-dependent signal from N-type Ca^{2+} channels to the SNARE proteins (23). The synprint site of P/Q type Ca^{2+} channels was also shown to interact with SNARE proteins (15), but the functional significance of the interaction in neurotransmitter release has not been demonstrated. The present study reveals that the synprint site of P/Q type Ca^{2+} channels is required for localization of newly synthesized channels to the nerve terminals of SCGNs. Mutant $Ca_v2.1$ channels with a deletion of the N-terminal half of the synprint site were fully functional, but they were not modulated by SNAP-25, were less effectively transported to nerve terminals than wild-type channels, and were less effective in initiating transmitter release. Mutant $Ca_v2.1$ channels having a deletion of the C-terminal half of the synprint site also were fully functional, but they were not modulated by SNAP-25, were much less effectively transported to nerve terminals, and their ability to initiate synaptic transmission was correspondingly reduced. Mutant $Ca_v2.1$ channels with a deletion of all of the synprint site were not functionally expressed and also were not effectively transported to nerve terminals. Thus, our results reveal an unexpected requirement for the synprint site for efficient nerve terminal localization of Ca^{2+} channels. This is likely to reflect a requirement for interaction of Ca^{2+} channels with SNARE proteins for successful assembly and incorporation into the specialized transport vesicles in the endoplasmic reticulum and Golgi apparatus that are destined for transport to the presynaptic terminal (e.g., refs. 24 and 25). We suppose that this requirement for association with SNARE proteins is permissive for Ca^{2+} channel localization in nerve terminals but does not provide the primary targeting information for nerve terminal localization because SNARE proteins are broadly distributed in neurons. A

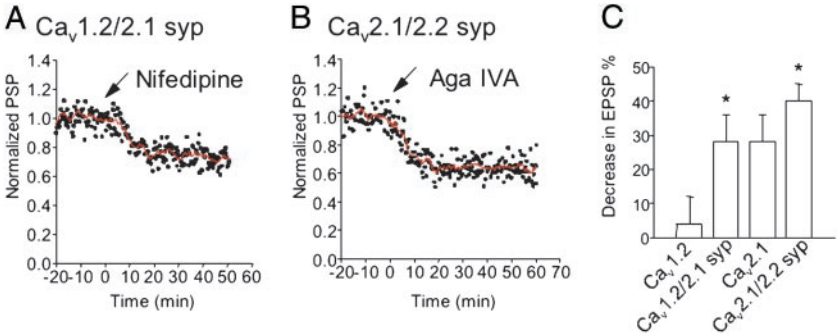

Fig. 6. Expression and function of chimera $Ca_v1.2/Ca_v2.1$ syp and $Ca_v2.1/Ca_v2.2$ syp. Synaptic transmission was recorded from pairs of SCGNs as described in *Experimental Procedures*, and nifedipine (2.5 μM) or ω-agatoxin IVA (250 nM) was applied at $t = 0$ (arrows). (*A*) EPSPs were recorded from synapses expressing the $Ca_v1.2$-synprint chimera ($n = 5$). (*B*) EPSPs were recorded from synapses expressing the $Ca_v2.1$-synprint chimera ($n = 6$). (*C*) Bar graph illustrating the mean EPSP values ± SEM 20 min after the toxin application. *, A statistically significant difference from control at $P < 0.05$ with Student's *t* test; syp, synprint.

NEUROSCIENCE

candidate for the primary targeting motif has been identified in the C-terminal domain of $Ca_v2.2$ channels. Amino acid sequences that interact with the PDZ domain protein MINT and the SH3 domain protein CASK have been shown to be required for nerve terminal targeting and capable of targeting heterologous proteins to the nerve terminal (26). Because association of presynaptic Ca^{2+} channels with SNARE proteins is required for their effective initiation of fast synaptic transmission (16, 17) and modulates their functional activity (22, 27, 28), preassembly with SNARE proteins before transport to the nerve terminal would assure that Ca^{2+} channels are fully prepared for physiological function in synaptic transmission on arrival at presynaptic sites. Additional sequences in the region of the synprint site may also provide independent targeting information for Ca^{2+} channel localization.

The synprint region of Ca^{2+} channels is not only required for nerve terminal localization, but it is also sufficient to allow functional expression of chimeric $Ca_v1.2/Ca_v2.1$ channels at nerve terminals, resulting in synaptic transmission initiated by L-type Ca^{2+} currents. These results indicate that the synprint site, perhaps along with additional nearby sequence elements in $L_{II\text{-}III}$, are sufficient to allow $Ca_v1.2$ to be transported to the nerve terminal and to function in synaptic transmission. Ca_v1 channels that conduct L-type Ca^{2+} currents are prominent in developing growth cones (29), so it is likely that they contain appropriate targeting information for nerve terminal localization in developing neurons, even though they do not have interaction sites for MINT and CASK (26). Targeting of Ca_v1 channels to mature synapses may be prevented by a requirement for SNARE protein binding and may be restored on insertion of a synprint site.

Exogenously expressed $Ca_v2.1$ channels are less effective in initiating synaptic transmission than endogenously expressed $Ca_v2.2$ channels (18). The synprint sites from $Ca_v2.1$ and $Ca_v2.2$ channels differ in their specificity and Ca^{2+} regulation of binding of SNARE proteins (15, 30). The synprint site from the rbA isoform of $Ca_v2.1$ used here specifically binds SNAP-25 independent of Ca^{2+}, whereas the synprint site from $Ca_v2.2$ binds both SNAP-25 and syntaxin comparably and has a sharp Ca^{2+}-dependence. Our results show that insertion of the synprint site from $Ca_v2.2$ channels in $Ca_v2.1/Ca_v2.2$ chimeras yields enhanced synaptic transmission initiated by P/Q-type Ca^{2+} currents. Thus, the synprint site, possibly together with other unidentified functional sequences nearby in $L_{II\text{-}III}$, can act in a positive manner to increase localization and function of Ca^{2+} channels in nerve terminals. The differences in SNARE protein binding between the rbA isoform of $Ca_v2.1$ and $Ca_v2.2$ may play a role in this difference in function in synaptic transmission. In addition, as shown previously (16, 17), interaction of the synprint site with SNARE proteins is required for fast, efficient synaptic transmission initiated by endogenous Ca^{2+} channels. Evidently, the synprint site is a multifaceted determinant of the unique ability of presynaptic Ca_v2 channels to initiate fast synaptic transmission.

We thank Ms. Elizabeth M. Sharp for support in the molecular biological experiments and Dr. Nathan Lautermilch for confirming the function of the $Ca_v1.2/Ca_v2.1$ syp chimera. This work was supported by grants from Human Frontier Science Program (to S.M.), the Japanese Ministry of Education, Science, Sports and Culture (to S.M.), the Japan Society for the Promotion of Science (to S.M.), the Medical Research Council of Canada (to H.Z.), National Institutes of Health Grant NS22625 (W.A.C., C.T.Y., R.E.W., S.J.M., and T.S.), and the Muscular Dystrophy Association (R.E.W.).

1. Dunlap, K., Luebke, J. I. & Turner, T. J. (1995) *Trends Neurosci.* **18,** 89–98.
2. Tsien, R. W., Lipscombe, D., Madison, D., Bley, K. & Fox, A. (1995) *Trends Neurosci.* **18,** 52–54.
3. Takahashi, M., Seagar, M. J., Jones, J. F., Reber, B. F. & Catterall, W. A. (1987) *Proc. Natl. Acad. Sci. USA* **84,** 5478–5482.
4. Hofmann, F., Lacinova, L. & Klugbauer, N. (1999) *Rev. Physiol. Biochem. Pharmacol.* **139,** 33–87.
5. Catterall, W. A. (1998) *Cell Calcium* **24,** 307–323.
6. Takahashi, T. & Momiyama, A. (1993) *Nature* **366,** 156–158.
7. Mochida, S., Saisu, H., Kobayashi, H. & Abe, T. (1995) *Neuroscience* **65,** 905–915.
8. Wu, L.-G., Westenbroek, R. E., Borst, J. G. G., Catterall, W. A. & Sakmann, B. (1999) *J. Neurosci.* **19,** 726–736.
9. Turner, T. J., Adams, M. E. & Dunlap, K. (1992) *Science* **258,** 310–313.
10. Wu, L. G., Borst, J. G. & Sakmann, B. (1998) *Proc. Natl. Acad. Sci. USA* **95,** 4720–4725.
11. Hirning, L. D., Fox, A. P., McCleskey, E. W., Olivera, B. M., Thayer, S. A., Miller, R. J. & Tsien, R. W. (1988) *Science* **239,** 57–61.
12. Sather, W. A., Tanabe, T., Zhang, J.-F., Mori, Y., Adams, M. E. & Tsien, R. W. (1993) *Neuron* **11,** 291–303.
13. Sheng, Z.-H., Rettig, J., Takahashi, M. & Catterall, W. A. (1994) *Neuron* **13,** 1303–1313.
14. Sheng, Z.-H., Rettig, J., Cook, T. & Catterall, W. A. (1996) *Nature* **379,** 451–454.
15. Rettig, J., Sheng, Z.-H., Kim, D. K., Hodson, C. D., Snutch, T. P. & Catterall, W. A. (1996) *Proc. Natl. Acad. Sci. USA* **93,** 7363–7368.
16. Mochida, S., Sheng, Z.-H., Baker, C., Kobayashi, H. & Catterall, W. A. (1996) *Neuron* **17,** 781–788.
17. Rettig, J., Heinemann, C., Ashery, U., Sheng, Z.-H., Yokoyama, C. T., Catterall, W. A. & Neher, E. (1997) *J. Neurosci.* **17,** 6647–6656.
18. Mochida, S., Westenbroek, R. E., Yokoyama, C. T., Itoh, K. & Catterall, W. A. (2003) *Proc. Natl. Acad. Sci. USA* **100,** 2813–2818.
19. Snutch, T. P., Tomlinson, W. J., Leonard, J. P. & Gilbert, M. M. (1991) *Neuron* **7,** 45–47.
20. Yokoyama, C. T., Westenbroek, R. E., Hell, J. W., Soong, T. W., Snutch, T. P. & Catterall, W. A. (1995) *J. Neurosci.* **15,** 6419–6432.
21. Hockerman, G. H., Johnson, B. D., Scheuer, T. & Catterall, W. A. (1995) *J. Biol. Chem.* **270,** 22119–22122.
22. Zhong, H., Yokoyama, C. T., Scheuer, T. & Catterall, W. A. (1999) *Nat. Neurosci.* **2,** 939–941.
23. Mochida, S., Yokoyama, C. T., Kim, D. K., Itoh, K. & Catterall, W. A. (1998) *Proc. Natl. Acad. Sci. USA* **95,** 14523–14528.
24. Zhai, R. G., Vardinon-Friedman, H., Cases-Langhoff, C., Becker, B., Gundelfinger, E. D., Ziv, N. E. & Garner, C. C. (2001) *Neuron* **29,** 131–143.
25. Ahmari, S. E., Buchanan, J. & Smith, S. J. (2000) *Nat. Neurosci.* **3,** 445–451.
26. Maximov, A. & Bezprozvanny, I. (2002) *J. Neurosci.* **22,** 6939–6952.
27. Bezprozvanny, I., Scheller, R. H. & Tsien, R. W. (1995) *Nature* **378,** 623–626.
28. Wiser, O., Bennett, M. K. & Atlas, D. (1996) *EMBO J.* **15,** 4100–4110.
29. Schindelholz, B. & Reber, B. F. (2000) *Eur. J. Neurosci.* **12,** 194–204.
30. Kim, D. K. & Catterall, W. A. (1997) *Proc. Natl. Acad. Sci. USA* **94,** 14782–14786.